PCCP
Physical Chemistry Chemical Physics

Accepted Manuscript

This article can be cited before page numbers have been issued, to do this please use: E. Dick, A. Fouda, N. A. Besley and P. Licence, *Phys. Chem. Chem. Phys.*, 2020, DOI: 10.1039/C9CP01297D.

This is an Accepted Manuscript, which has been through the Royal Society of Chemistry peer review process and has been accepted for publication.

Accepted Manuscripts are published online shortly after acceptance, before technical editing, formatting and proof reading. Using this free service, authors can make their results available to the community, in citable form, before we publish the edited article. We will replace this Accepted Manuscript with the edited and formatted Advance Article as soon as it is available.

You can find more information about Accepted Manuscripts in the Information for Authors.

Please note that technical editing may introduce minor changes to the text and/or graphics, which may alter content. The journal's standard Terms & Conditions and the Ethical guidelines still apply. In no event shall the Royal Society of Chemistry be held responsible for any errors or omissions in this Accepted Manuscript or any consequences arising from the use of any information it contains.

View Article Online
DOI: 10.1039/C9CP01297D

Probing the Electronic Structure of Ether Functionalised Ionic Liquids Using X-ray Photoelectron Spectroscopy

*Ejike J. Dick,[1,2] Adam E. A. Fouda,[1] Nicholas A. Besley[1] and Peter Licence[1,2]**

[1]School of Chemistry, The University of Nottingham, Nottingham NG7 2RD, UK

[2]The GSK Carbon Neutral Laboratory, The University of Nottingham Innovation Park, Triumph Road, Nottingham NG7 2TU, UK

**To whom correspondence should be addressed:*

peter.licence@nottingham.ac.uk

Tel: +44 115 8466176

DOI: 10.1039/C9CP01297D

Abstract

The charge distribution associated with individual components in functionalised ionic liquids (ILs) can be tuned by careful manipulation of the substituent groups incorporated into the ions. Here we use X-ray photoelectron spectroscopy to investigate the impact of substituent atoms on the electronic structure of similar imidazolium-based systems each paired with a common anion, $[Tf_2N]^-$. The experimental measurements revealed an unexpected variation in the charge density distribution within the IL cation when the oxygen atom in a poly-ether containing side chain is moved by just one atomic position. This surprising observation is supported by density functional theory calculations.

Introduction

X-ray photoelectron spectroscopy (XPS) is an established and commonly applied surface analysis technique,[1-3] which in the recent past, has been employed extensively in the study of ionic liquid-based systems.[4-8] As a general statement, XPS can provide detailed information about the electronic environment, and charge distribution associated with individual components at, or near to, the surface of a material. High-level atomistic data can be used to inform the design of more efficient processes, by delivering insight into local surface composition and orientation,[4, 5, 9] and complex interactions that can exist between charge carriers and solutes alike.[10-13] Continued structural modification and the inclusion of targeted functionalities and motifs that enable hydrogen bonding or recognition can deliver highly functionalised performance molecules or so-called "designer solvents".[14,15-17]

The polyethylene (PEG) moiety was initially grafted into the cationic and anionic components of ILs to yield ion-conducting polymers for electrochemical applications.[18, 19] Since then, the relevance of ether-functionalised ILs has grown, with the materials demonstrating great potential for sustainable chemical applications.[20] For instance, PEG can be naturally derived from biorefinery and plant waste *via* solvolysis of soft wood biomass,[20] or the catalytic conversion of cellulose into ethylene glycol and ethylene glycol monoethers.[21] Improved catalytic performance and reduced viscosities, when compared to alkyl substituted analogues, is also noted.[14, 22-27] Ether and PEG substituted systems now find application as alternative solvents or performance molecules across multiple aspects of science, technology and engineering,[28-33] including, for example, as catalyst for the synthesis of butyl acetate and subsequent esterification of carboxylic acid,[22, 23] for selective CO_2 capture,[34] and as anti-wear additives to improve tribological performance.[32, 33]

View Article Online
DOI: 10.1039/C9CP01297D

Early XPS studies of PEG-functionalized systems have largely focused upon the orientation of surface structure of imidazolium-based systems,[7, 10, 35] and were completed out using non-monochromatic X-ray sources which sometimes suffer from reduced resolution of primary XP photoemission envelopes. A recent study, of surface enrichment in equimolar mixtures of non-functionalised and ether-functionalised imidazolium-based ILs, by Heller *et al.,*[36] showed that the electronic structure of the aromatic region of the imidazolium cation is shifted to a significantly higher electron binding energies (BEs) when compared to $[C_8C_1Im]^+$, when the ether oxygen is directly bound to the imidazolium charge carrier. Here we demonstrate how the use of a higher resolution, monochromated, X-ray source can reveal subtle new insights which can inform the design of next generation reaction systems and alternative solvents. In this contribution we utilize XPS and density functional theory (DFT) based BE calculations to evaluate intra-molecular interaction between the polyether oxygen and the imidazolium charge carrier group. We show that by manipulation of the position of the oxygen atom, nearest to the cationic charge carrier, we can tune the electronic properties of the resulting ionic liquid in a very delicate way. The relative positioning of the oxygen atom can have a marked impact upon on the immediate side chain chemistry of the IL, while exhibiting minimal impact on the imidazolium ring itself. This observation, although subtle in isolation, manifests as a distinct change in the overall profile of the C1s photoemission envelope which is easily recognized by inspection. Responding to this observation, we also propose a modified deconstruction model for ether containing systems, the detail of which is underpinned by the DFT calculations and modelling.

To assist in the development and description of these data, we propose a relatively simple nomenclature system which is designed to minimize ambiguities when visualising structures. The system is defined by short hand notations ascribed to each N-based substituent in turn. Structures studied herein include functionalised substituents, so our descriptor for the complex substituent must reflect this. If we apply the same logic, we can develop a descriptor for each substituent in turn, see **Figure 1** and **Table 1** for IL structures and linked nomenclature.

View Article Online
DOI: 10.1039/C9CP01297D

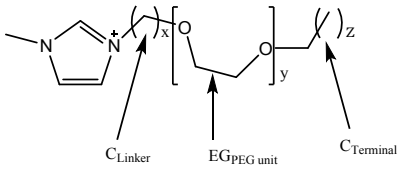

$[(CxEGyC_Z)C_1Im]^+$

i.e

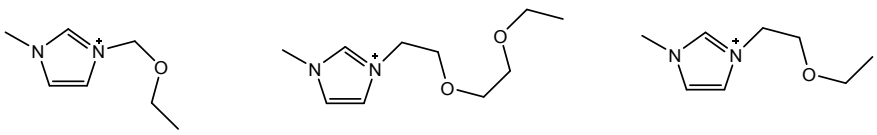

$[(C_1OC_2)C_1Im]^+$ β–IL

$[(C_2EG_1C_2)C_1Im]^+$ γ–IL

$[(C_2OC_2)C_1Im]^+$ γ–IL

Figure 1: *Nomenclature system adopted for functionalised ionic liquids studied in this work*

Table 1: Structures and Abbreviation of Ionic Liquids investigated

Abbreviation	Structure	Name
$[C_4C_1Im][Tf_2N]$	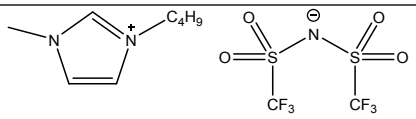	3-butyl-1-methylimidazolium bis(trifluoromethanesulfonyl)imide
$[(C_1OC_2)C_1Im][Tf_2N]$ (β-IL)	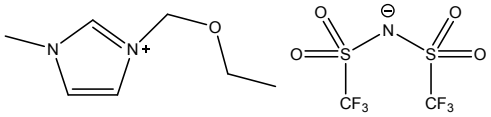	3-(ethoxymethy)-1,-methylimidazolium bis(trifluoromethanesulfonyl)imide
$[(C_1OC_2)C_1Im][Tf_2N]$ (Methylated β-IL)	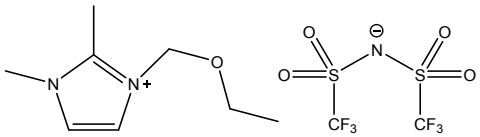	3-(ethoxymethyl)-1,2-dimethylimidazolium bis(trifluoromethanesulfonyl)imide
$[(C_2OC_2)C_1Im][Tf_2N]$ (γ-IL)	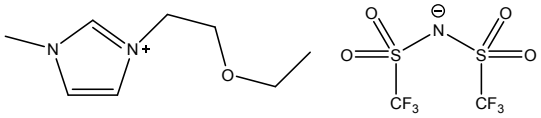	3-(2-ethoxyethyl)-1-methylimidazolium bis(trifluoromethanesulfonyl)imide
$[(C_2OC_2)C_1C_1Im][Tf_2N]$ (Methylated γ-IL)	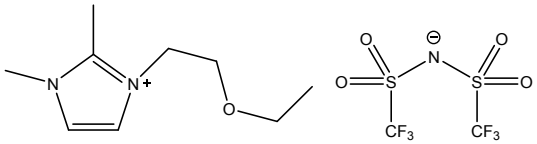	3-(2-ethoxyethyl)-1,2-dimethylimidazolium bis(trifluoromethanesulfonyl)imide

View Article Online
DOI: 10.1039/C9CP01297D

Experimental

Materials Preparation: All ionic liquids reported were synthesized in our laboratory using slightly modified procedures based upon those reported in the literature.[7, 37] Unless stated, precursors were purchased from Sigma Aldrich or Alfa and used without further purification. Functionalized ILs were prepared by direct alkylation of the methyl imidazole with the respective alkyl halide. All compounds were dried *in vacuo* ($p \leq 10^{-6}$ mbar) at between 50-70°C and stored under argon prior to analysis by NMR, ^{1}H (400 MHz), ^{13}C (101 MHz), and ^{19}F (377 MHz) spectra were recorded at room temperature in dimethyl sulfoxide-d_6 (deuterated DMSO) on a Bruker AV 400. Mass Spectrometry (ESI-MS) were recorded with Bruker MicroTOF 61 spectrometer, XPS data collected using Kratos Axis Ultra spectrometer. CHN/micro analysis was obtained using Exeter CE-440 Elemental Analyser. Full data, including methods of synthesis and all XPS spectra-deconstruction model for materials investigated, as well as instrument calibration, data collection and data analysis are available in the ESI.

Ionic Liquid Purity: At the outset, by inspection of the survey scans associated with each sample (available in the ESI), it can be quickly established that the samples are all of high purity, *i.e.* only elements expected in the molecular formulae are observed. The data confirms the absence of residual halides and more importantly silicone impurities originating from laboratory grease or similar contaminants which can surface segregate and influence surface composition and chemistry. In terms of composition, the elemental data shows a good agreement between experimental and nominal stoichiometries, with all samples below the 10 % within acceptable experimental error, **(Table 2)**. Ion chromatography measurement confirmed that residue halide and/or metal impurities derived from salt exchange chemistries were below detection limits.

Density Functional Theory (DFT): The structure was optimized using density functional theory with the B97-1 exchange-correlation functional,[38] and the pcSseg-1 basis set.[39] The structural model utilized for the calculations consist of the cation with two counterions placed near the imidazole ring, these structures are shown in the ESI. The electron BEs were computed using a Δself-consistent field (ΔSCF) approach,[40] with the PBE functional,[41] and larger pcSseg-2 basis set. These basis sets have been shown to be accurate for the calculation of core-ionisation energies.[42] These calculations used the optimised trimer structure in conjunction with the polarised continuum model (PCM),[43-45] with a dielectric constant of 15.0 to capture long range electrostatic effects.

Table 2 Quantitative analysis of XP spectra for the PEG functionalized ionic liquids studied. Measured experimental and nominal (in brackets) stoichiometries in number of atoms. Associated error in the experiment is of the order ± 10 %

		% Composition				
		C 1s	O 1s[a]	N 1s	F 1s	S 2p
Ionic Liquid	RSF[6, 46]	0.278	0.780	0.477	1.000	0.668
$[C_4C_1Im][Tf_2N]$		10.0 (10)	3.9 (4)	2.9 (3)	6.1 (6)	1.8 (2)
$[C_8C_1Im][Tf_2N]$		14.6 (14)	3.9 (4)	3.1 (3)	5.9 (6)	1.9 (2)
$[(C_1OC_2)C_1Im][Tf_2N]$, β-IL		9.2 (9)	4.8 (5)	2.8 (3)	6.1 (6)	1.8 (2)
$[(C_1OC_2)C_1C_1Im][Tf_2N]$		10.3 (10)	4.7 (5)	3.0 (3)	5.9 (6)	1.9 (2)
$[(C_2OC_2)C_1Im][Tf_2N]$, γ-IL		10.4 (10)	4.6 (5)	2.9 (3)	6.0 (6)	1.9 (2)
$[(C_2OC_2)C_1C_1Im][Tf_2N]$		11.2 (11)	4.8 (5)	3.0 (3)	5.9 (6)	1.8 (2)

Table 3: Electron binding energies (in eV) for the ionic liquids studied. The associated experimental error is of the order ±0.1 eV. Charge correction is achieved indirectly by setting the value of the F 1s equal to that observed in a standard reference material, $[C_8C_1Im][Tf_2N]$, previously referenced to 285.0 eV.[47]

	Binding Energy / eV													
	Cation									Anion				
Ionic Liquids	$C_{aliphatic}$ 1s	C_{hetero} 1s	$C_{4,5}$ 1s	C_2 1s	C_7 1s	C_{11} 1s	C_{12} 1s	N_{cat} 1s	O_{cat} 1s	C_{CF_3} 1s	N_{ani} 1s	O 1s[a]	F 1s	S 2 $p_{3/2}$
$[C_4C_1Im][Tf_2N]$[b]	285.2	286.6	287.1	287.6	-	-	-	402.1	-	293.0	399.4	532.6	688.8	169.0
$[C_8C_1Im][Tf_2N]$[c]	285.0	286.6	287.1	287.7	-	-	-	402.1	-	292.9	399.4	532.6	688.8	168.9
$[(C_1OC_2)C_1Im][Tf_2N]$, β-IL	285.1	286.5	287.0	287.7	288.3	-	-	402.0	533.5	292.8	399.4	532.6	688.8	168.8
$[(C_1OC_2)C_1C_1Im][Tf_2N]$	285.2	286.5	286.9	287.9	288.3	286.1	-	401.9	533.4	292.8	399.4	532.6	688.8	168.8
$[(C_2OC_2)C_1Im][Tf_2N]$, γ-IL	285.1	286.5	287.1	287.7	-	-	-	402.0	-	292.9	399.4	532.7	688.8	168.9
$[(C_2OC_2)C_1C_1Im][Tf_2N]$	285.0	286.5	287.0	287.8	-	-	286.0	401.9	-	292.8	399.3	532.6	688.8	168.8

a = BE value for O 1s from the polyether chain in the cation, and the sulfonyl oxygen from the $[Tf_2N]^-$

b and c = Alkyl substituted ionic liquids reference materials, n = 4 and 8

View Article Online
DOI: 10.1039/C9CP01297D

Comparison of the Photoemission Envelopes for β and γ-substituted Ether-functionalized Ionic liquids.

The high resolution C1s photoemission envelopes for two imidazolium-based ionic liquids, with an oxygen atom positioned at either the β or γ position of the longest substituent side chain are shown in **Figure 2**.

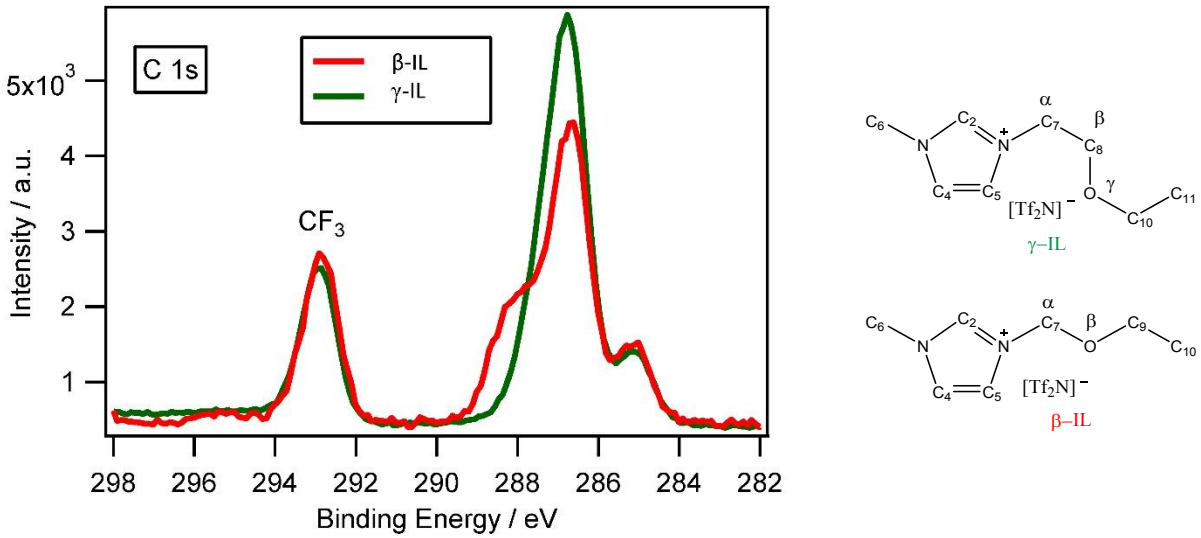

Figure 2: *Overlaid C 1s high resolution spectra for γ-IL, $[(C_2OC_2)C_1Im][Tf_2N]$ (green) and β-IL, $[(C_1OC_2)C_1Im][Tf_2N]$ (red), highlighting significant higher binding energy shift and difference in photoemission intensity. Note, the number of atoms in γ-IL is one carbon greater than that of β-IL and the intensities are normalized to the area of the C_{CF_3} 1s in γ-IL. Charge correction for both ILs was achieved indirectly by setting the value of the F 1s photoemission equal to that observed in a standard reference material, (F = 688.8 eV).*[47]

It is clear, simply by inspection, that the photoemission line shapes for the ILs are noteably different, β-IL (red line) has a clear shoulder at approximately ~288 eV. This striking impact on the photoemission envelope is so pronounced that it motivated the need for further interrogation. On a structural level, by moving the O atom, by just a single atom position closer to the imidazolium charge carrier, in the substituent chain could have a notable impact in the electronic structure, and potentially influence point charge distribution around the cation itself.

In order to establish which carbon atoms in the structure are impacted to the greatest extent, and to consider if this observation could be used in the design and engineering of solvents on the molecular level, the establishment of a new peak deconstruction for similar functionalised systems is needed. However, this requires further analysis to firmly establish which individual carbon components were being influenced most directly by the change in proximity of the oxygen atom.

View Article Online
DOI: 10.1039/C9CP01297D

A close analysis of the overlaid XP high resolution photoemission spectra of β-IL and γ-IL (**Figure 2)** shows an apparent reduction in photoemission intensity, as well as significant reduction of the FWHM of the photoemission XP profile for β-IL, relative to γ-IL. The reduction correlates to a shift of a single methylene unit (CH_2), within the substituent group from (C-O), at ~ 286.5 eV, to a more electron deficient environment (N-CH_2-O), at ~ 288.3 eV. The above analysis therefore, strongly suggests that the electronic structure of the C_7 1s component for β-IL was significantly impacted by switching the ether O position from γ to β. Also, this data can be directly correlated to the degradation temperature, T_d values previously determined for both β and γ-ILs, at 262.8 °C and 285.2 °C respectively,[48] in which the authors suggested that their thermal stability is strongly dependent on the methylene spencer length. While pyrolysis of β-IL at 262.8 °C revealed a synergistic electron-withdrawal effect of N^+ and O atoms adjacent to the CH_2 spencer, hence, better reactivity for β-IL.

In-depth analysis of these data was performed to establish the particular carbon atom within the cation is mostly impacted, as well as to establish whether there is interaction between the ether O and the imidazolium cationic headgroup. An analysis of the electronic structure of the N_{cation} 1s region (which is directly bound to the C_2 1s and $C_{4,5}$ 1s components, within the imidazolium aromatic region), for both β-IL and γ-IL was carried out by comparing their binding energy with that observed for alkyl substituted IL, [C_4C_1Im][Tf_2N] (**Figure 3a**). The XP data revealed that the N 1s component in the three ILs investigated exhibited similarity in binding energy, suggesting that the electronic structure of the N 1s component for β-ILs is not significantly perturbed relative to γ-IL and [C_4C_1Im][Tf_2N]. This data can also be interpreted as minimal impact of the ether O on all components within the aromatic region of the imidazolium cation, for β-IL, including C_2 1s, $C_{4,5}$ 1s and N 1s. This is also true for other longer chain PEG-functionalised ILs [($C_2EG_1C_2$)C_1Im][Tf_2N] and [($C_2EG_2C_2$)C_1Im][Tf_2N] (structure provided in ESI), where polyether O is substituted at γ position.

View Article Online
DOI: 10.1039/C9CP01297D

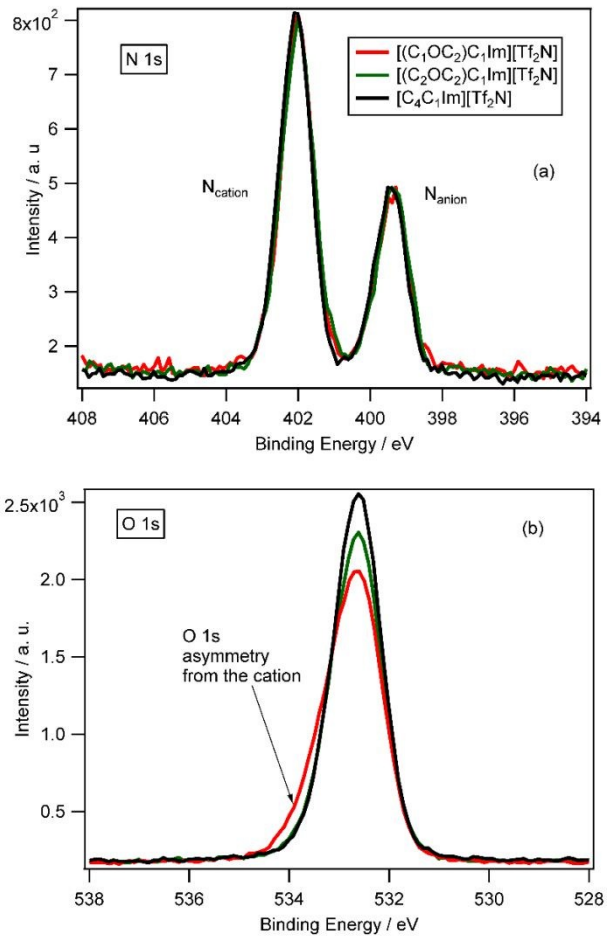

Figure 3: *(a), N 1s high resolution spectra for β-ILs, [(C$_1$OC$_2$)C$_1$Im][Tf$_2$N] (red), γ-IL, [(C$_2$OC$_2$)C$_1$Im][Tf$_2$N] (green), and [C$_4$C$_1$Im][Tf$_2$N],(blue), showing the similarity in binding energy of the N$_{cation}$ 1s component of the three ionic liquids. (b) O 1s high resolution spectra for β-ILs, red, γ-IL, green, and [C$_4$C$_1$Im][Tf$_2$N], blue, showing asymmetry in the photoemission spectra for β-IL. Intensity normalized to the area of the N$_{cation}$ 1s for γ-IL.*

Similarly, a review of the O 1s region for β-IL revealed an asymmetry at ~533.5 eV, **Figure 3b**. This binding energy is much higher than those observed for the γ-IL and alkyl substituted ILs, *i.e* 532.6 eV for both ILs, with a binding energy difference, (ΔBE) equal to 0.9 eV. This is significantly higher than the experimental error and similar to those observed in a range of polymers.[49] Since O is both present in the cation and the anion, the higher BE shift is more likely from the ether O in the cation, as O from the $[Tf_2N]^-$ for γ-IL exhibits coincidental BE values, which could not be separately resolved by our spectrometer, thus indicative of similarity in electronic structure. This observation is in line with previous XPS measurement of ether functionalised systems.[7, 10] This is also in line with the DFT data calculated for cationic polyether O and anionic O from the $[Tf_2N]^-$ for both ILs, in which the BE for O in γ-IL ions has no significant difference whereas a significant difference was observed for the O in the β-

IL ions. (DFT data is provided in the ESI, Table SI 2 and 3). This observation can be correlated to the density (ρ) of the two ILs. Although ρ is a bulk measurement parameter, it strongly correlates to intra and intermolecular interaction as well as packing efficiency of ILs.[50] Hence the previously measured ρ for both β and γ-ILs at 1.5015 g $cm^{-3}$and 1.4577 g cm^{-3} respectively,[48] was described by the authors as dependent on the structure of the cation, including ether chain length. While other studies of different N-based ether functionalised ILs correlated ρ to the electronic structure of the ionic liquid cation.[51, 52] Other physiochemical properties in which both β-IL and γ-ILs have been shown to demonstrate marked differences includes viscosity at 57.0 cP and 46.4 cP respectively,[48] and surface tension as β-IL (34.24 mN m^{-1}) *vs* γ-IL (33.61 mN m^{-1}).[48] While melting point (T_m) for γ-IL was observed to be -7.6 °C, but was not observed for β-IL at the same temperature.[48] Other studies where slight variation in methylene spencer unit in ether functionalised ILs led to significant changes in electrochemistry,[14, 53, 54] density,[55] viscosity,[53] and T_d,[29, 55] have also been published.

To further investigate the incidence of intramolecular interactions a series of DFT calculations was executed, all of which suggest that no significant interaction was observed, thus supporting the XPS data (**Figure 4a and b**)

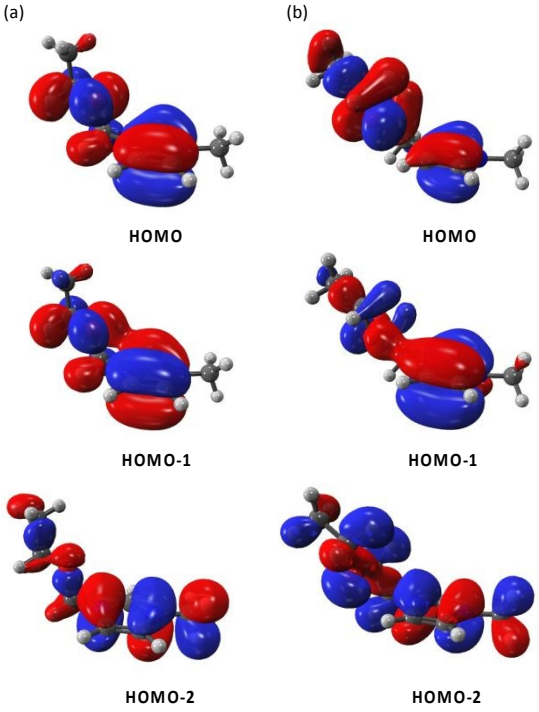

Figure 4. *Molecular orbitals of (a) β-IL, $[(C_1OC_2)C_1Im]^+$ and (b) γ-IL, $[(C_2OC_2)C_1Im]^+$ illustrating the overlap of the p orbital on oxygen with the π orbitals of the imidazolium ring.*

Figure 4 shows the three highest occupied molecular orbitals (HOMOs) for the β and γ-ILs. These orbitals represent the π molecular orbitals of the imidazolium ring and can provide some insight into the weak interaction between the oxygen and imidazolium ring that is observed for both of these ILs. For both of these ILs there is little overlap between the p-type orbitals localised on the oxygen and the p orbitals of the ring owing to both the distance of the oxygen atom from the ring and also its alignment with respect to the imidazolium ring. Crucially for the β-IL where the oxygen is closer to the ring, the oxygen does not lie in the plane of the imidazolium which means that it cannot form part of a delocalised π molecular orbital spanning the imidazolium ring and the ether oxygen, and this is the case for both the β and γ-ILs. As a consequence, there is only a small interaction between the oxygen and the imidazolium ring for both of these ILs.

In order to firmly establish that the C_7 1s component is mostly impacted within the β-IL, the C_2 position was methylated, hence turning off hydrogen bonding interaction within the site, and distorting charge transfer between the C_2 and other potential interaction sites.[56-58]

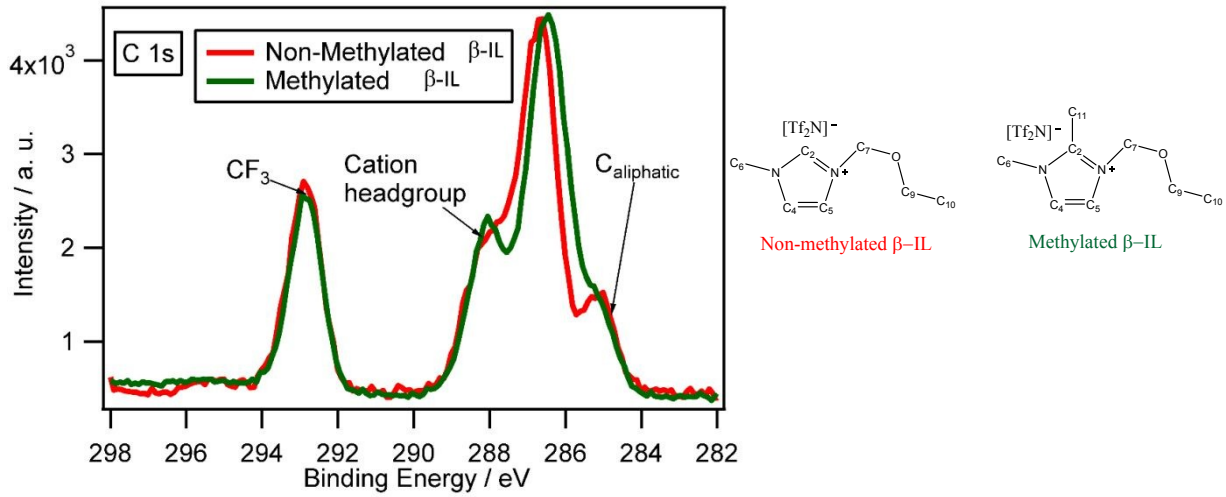

***Figure 5**: Overlaid C 1s high resolution XP spectra for non-methylated (red) and methylated (green) β-IL, $[(C_1OC_2)C_1Im][Tf_2N]$ and $[(C_1OC_2)C_1C_1Im][Tf_2N]$ respectively. Intensity normalized to the area of the C_{CF_3} 1s for non-methylated β-IL, $[(C_1OC_2)C_1Im][Tf_2N]$. Charge correction is achieved indirectly by setting the value of the F 1s photoemission equal to that observed in a standard reference material $[C_8C_1Im][Tf_2N]$, (F = 688.8 eV).[47]*

Inspection of the overlaid spectra for both ILs, (**Figure 5**), reveals there is an apparent broadening of the region with the highest intensity for the methylated β-IL (green colour) at ~286.0 eV. This is indicative of the presence of the methyl group directly bonded to the C_2 carbon. While the region with the highest binding energy (~288.5 eV) exhibited good alignment

between the two XP spectra. This suggests that the C_2 1s component in both ILs are in the same electronic environment, and independent of the methylation at the C_2 position. This data has therefore established the fact that the electronic structure of the C_2 1s component is not impacted by substituting polyether oxygen at β position to the imidazolium ring.

Table 4. Electron binding energies from XPS measurements and DFT calculations for the C_2, C_7. N_{cation} and O_{cation} components for non-methylated and methylated β and γ-ILs

$[(C_1OC_2)C_1Im][Tf_2N]$ (β-IL)			$[(C_2OC_2)C_1Im][Tf_2N]$ (γ-IL)		
XPS / eV	Cationic Components	DFT / eV	XPS / eV	Cationic Components	DFT / eV
287.7	C_2	290.7	287.7	C_2	290.7
288.3	C_7	291.4	286.5	C_7	290.1
402.0	N_{cation}	405.4	402.0	N_{cation}	405.3
533.5	O_{cation}	536.3	532.7	O_{cation}	536.0
$[(C_1OC_2)C_1C_1Im][Tf_2N]$ (Methylated β-IL)			$[(C_2OC_2)C_1C_1Im][Tf_2N]$ (Methylated γ-IL)		
287.9	C_2	291.1	287.7	C_2	291.1
288.3	C_7	291.5	286.5	C_7	290.1
401.9	N_{cation}	405.3	401.9	N_{cation}	405.3
533.4	O_{cation}	536.3	532.6	O_{cation}	536.0

A direct comparison of experimentally determined and calculated (DFT) BEs is presented in **Table 4,** as a general comment the absolute values, calculated by DFT are systematically higher than the experimental values. This difference can be attributed to the exchange-correlation functional and basis set used. Furthermore, the finite structural model used is likely to underestimate the long-range electrostatic interactions. However, these effects will be constant for the different systems, and crucially the trends in the computed BEs are in good agreement with the experimental data. The electronic structure of the cation and indeed the trimer model, which included one cation in the field of two anions, embedded in a continuum dielectric was chosen to provide a more reasonable description of the cation than would be provided by evaluation of a dimer pair (neutral ion pair) model. In particular, the calculations confirm that the C_7 1s component for the non-methylated and methylated β and γ-ILs exhibits higher BEs in comparison to the C_2 1s. The calculations also confirm that the electronic structure of the N_{cation} 1s for β-IL is perturbed to a lesser extent, when compared to a notable impact upon the BE of the O_{cation} 1s component in the β-IL.

Towards a Refined C1s Deconstruction Model for Ether-functionalized Imidazolium-based Ionic liquids

The systematic analysis of both β-IL and γ-IL demonstrates that their electronic structure is distinctively different, as a result, a new fitting model is required to correctly deconstruct the C 1s environment for β-IL. Consequently, the C 1s environment for γ-IL was deconstructed based upon the fitting model established for imidazolium-based alkyl substituted ILs.[6, 8, 47, 57, 59] (**Figure 6a).**

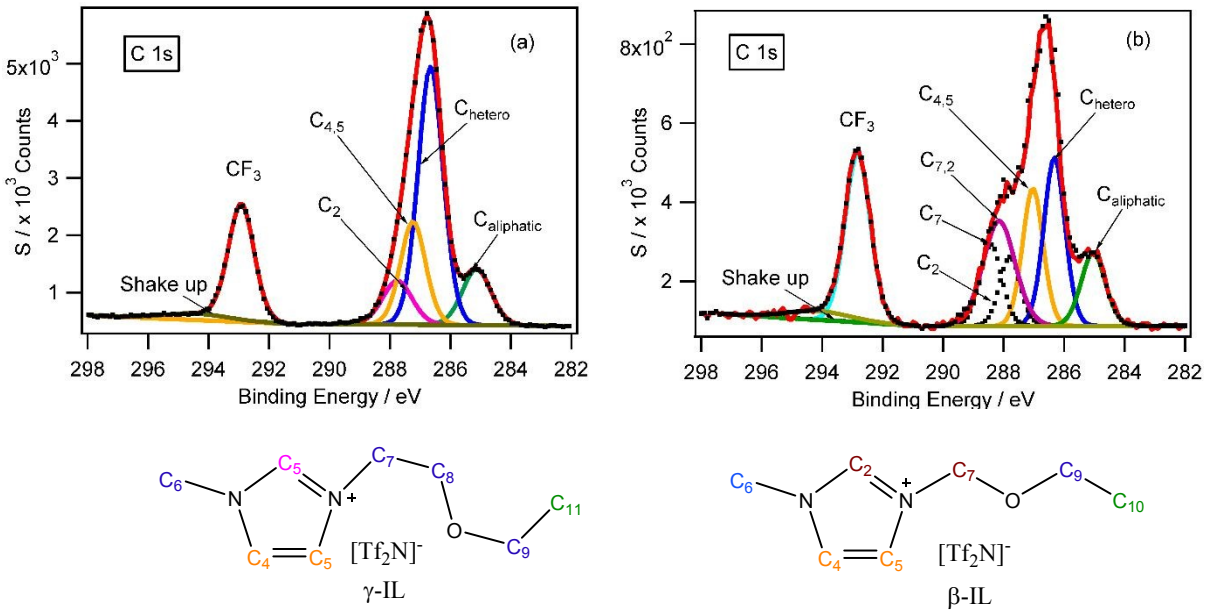

Figure 6*: C 1s XP high resolution spectra for γ-IL, [(C₂OC₂)C₁Im][Tf₂N] (a) and β-IL, [(C₂OC₁)C₁Im][Tf₂N] (b) showing four component deconstruction model used to describe the IL (where component at ~288.0 eV comprised of C₇ and C₂ 1s represented by dotted lines). Colour coded based on the different C 1s environment inherent in the systems. Charge correction is achieved indirectly by setting the value of the F 1s photoemission equal to that observed in a standard reference material [C₈C₁Im][Tf₂N], (F = 688.8 eV).*[47]

The C 1s component for both β-IL and γ-ILs were fitted based upon data obtained from XPS and DFT calculations. Parameter constraints was employed in both cases to achieve a reliable fit. This include constraining the FWHM to between 0.8 – 1.2 eV,[47] while area constraints was carried out in line with the stoichiometry of the ILs. Detailed parameter description used to fit the ILs is provided in the ESI (Table SI 1.1). After accounting for shake up/off phenomena which affects ~ 20 % of all photoemissions originating from the aromatic region of the imidazolium cation, the relative peak ratio for the four components in β-IL and γ-ILs is set at 1.8 : 1.6 : 2 : 1 for components C_{2+7} : C_{4+5} : C_{hetero} : $C_{aliphatic}$ and 0.8 : 1.6 : 4 : 1 for components C_2 : C_{4+5} : C_{hetero} : $C_{aliphatic}$ respectively. In the model, for γ-IL, the component from the CF_3

group of the $[Tf_2N]^-$ was fitted to the highest BE at 292.9 eV. This was followed by the C_2 1s component, directly bound to two electronegative N atoms within the imidazolium ring, at 287.7 eV, then the C_4 and C_5, which are both bound to one N atom within the imidazolium ring at 287.1 eV. The C atoms directly bound to an electronegative atom (N or O), outside the ring *i.e* C_{hetero} 1s atoms, comprising C_6, C_7, C_8 and $C_{10,}$ was fitted to 286.5 eV. While the terminal carbon which is involved in a C-C aliphatic type bond is fitted to 285.1 eV. The model for β-IL was fitted in line with the description above for the γ-IL (**Figure 6b**). The component at ~ 288.0 eV (with apparent broad FWHM) was fitted to accommodate the two most electron poor components C_7 1s and C_2 (dotted lines) at 288.3 eV and 287.7 eV respectively, thus supporting our hypothesis of the emergence of a new electron deficient component occasioned by altering the position of the ether O from the γ to β position.

Conclusions

The designer aspect of ionic liquids was exploited to graft polyether groups into IL structural framework, thus creating an opportunity to investigate fundamental interactions within the IL, using XPS. Although XPS studies of ether-functionalised systems have been previously undertaken, the effect of structural changes to IL ether substituent on fundamental intramolecular interaction within the system, has not been analysed in great depth. This work addresses this knowledge gap, in which the use of monochromated XPS provided the opportunity to further probe subtle intra-molecular interaction and electron density distribution within ether-functionalised systems.

A systematic investigation of two distinct ether functionalised systems suggests that the electronic structure of the imidazolium cation can be significantly perturbed by tuning the position of the polyether oxygen in the ether substituent. This can have profound impact on ionic liquid interaction with solvents and solute, for example, IL-catalyst interaction and dissolution of solutes. From our data, it was apparent that tuning the position of the polyether oxygen from γ to β position, results in highly electropositive substituent groups (C_7 1s and $O_{cations}$ 1s) for β-IL, in comparison to that observed for γ-IL. Interestingly, the electronic structure of the components within the aromatic region of the imidazolium cation headgroup (C_2 1s, $C_{4,5}$ 1s and N_{cation} 1s) for the β-IL were not perturbed as they recorded binding energy values similar to their γ-ILs counterparts. This data is inline with earlier studies of the physicochemical properties of these ILs in which they have been shown to exhibit significant difference in glass transition temperature, T_g, thermal decomposition temperature, T_d, viscosity, surface tension and density.[48]

The above XPS data was supported by DFT core-electron binding energy calculations which showed excellent agreement with the experimental observations. The C 1s environment for β-IL was consequently fitted based upon the data obtained from both XPS experiment and DFT calculation.

This data has provided critical insight that can aid the design of new materials with specific properties that can potentially impact hydrogen bonding, both intermolecularly and intramolecularly. This study has added to the depth of information already established for ether-functionalised systems that are useful in underpinning the development of new materials for specific chemical applications, including catalysis, dissolution and metal extraction.

Acknowledgements

We thank the EPSRC (EP/K005138/1, EP/P013341/1) for financial support and for provision of the Ionic Liquids XPS Facility and to The Leverhulme Trust for funding a studentship for AEAF (RPG-2016-103). We gratefully acknowledge the Nottingham NMRC for managing and maintaining the XPS instrumentation. EJD acknowledges the University of Nottingham for financial support.

References

1. D. Briggs, *Practical Surface analysis by X-ray Photoelectron Spectroscopy*, Wiley-Blackwell, 1983.
2. S. Hüfner and G. K. Wertheim, *Phys. Lett.*, 1975, **51**, 299-300.
3. G. Beamson and D. Briggs, *Mol. Phys.*, 1992, **76**, 919-936.
4. S. Caporali, U. Bardi and A. Lavacchi, *J. Electron Spectrosc.*, 2006, **151**, 4-8.
5. E. F. Smith, I. J. Villar-Garcia, D. Briggs and P. Licence, *Chem. Commun.*, 2005, 5633-5635.
6. E. F. Smith, F. J. M. Rutten, I. J. Villar-Garcia, D. Briggs and P. Licence, *Langmuir*, 2006, **22**, 9386-9392.
7. K. R. J. Lovelock, C. Kolbeck, T. Cremer, N. Paape, P. S. Schulz, P. Wasserscheid, F. Maier and H.-P. Steinrück, *J. Phys. Chem*, 2009, **113**, 2854-2864.
8. K. R. J. Lovelock, I. J. Villar-Garcia, F. Maier, H.-P. Steinrück and P. Licence, *Chem. Rev.*, 2010, **110**, 5158-5190.
9. J. Gottfried, M. Maier, F. Rossa, J. Gerhard, D. Schulz, P. S. Wasserscheid and H.-P. Steinrück, *Phys. Chem. Chem Phys.*, 2006, **220**, 1439-1453.
10. F. Maier, T. Cremer, C. Kolbeck, K. R. J. Lovelock, N. Paape, P. S. Schulz, P. Wasserscheid and H.-P. Steinrück, *Phys. Chem. Chem. Phys.*, 2010, **12**, 1905-1915.
11. S. Men, K. R. J. Lovelock and P. Licence, *Phys. Chem. Chem. Phys.*, 2011, **13**, 15244-15255.

12. I. J. Villar-Garcia, S. Fearn, G. F. De Gregorio, N. L. Ismail, F. J. V. Gschwend, A. J. S. McIntosh and K. R. J. Lovelock, *Chem. Sci.*, 2014, **5**, 4404.
13. S. Men, D. S. Mitchell, K. R. J. Lovelock and P. Licence, *Chemphyschem*, 2015, **16**, 2211-2218.
14. S. K. Tang, G. A. Baker and H. Zhao, *Chem. Soc. Rev.*, 2012, **41**, 4030-4066.
15. I. Newington, J. M. Perez-Arlandis and T. Welton, *Org. Lett.*, 2007, **9**, 5247-5250.
16. A. E. Visser, R. P. Swatloski, W. M. Reichert, R. Mayton, S. Sheff, A. Wierzbicki, J. H. Davis and R. D. Rogers, *Chem. Commun.*, 2001, 135-136.
17. Y. L. Hu, *Progress and Developments in Ionic Liquids*, 2017, 185-212.
18. M. Armand, F. Endres, D. R. MacFarlane, H. Ohno and B. Scrosati, *J. Nat. Sci.*, 2009, **8**, 621-629.
19. Y. Nakai, K. Ito and H. Ohno, *Solid State Ionics*, 1998, **113**, 199-204.
20. T. T. Nge, Y. Tobimatsu, S. Takahashi, E. Takata, M. Yamamura, Y. Miyagawa, T. Ikeda, T. Umezawa and T. Yamada, *Acs Sustain. Chem. Eng.*, 2018, **6**, 7841-7848.
21. J. X. Xi, D. Q. Ding, Y. Shao, X. H. Liu, G. Z. Lu and Y. Q. Wang, *Acs Sustain Chem. Eng.*, 2014, **2**, 2355-2362.
22. A. H. Jadhav, K. Lee, S. Koo and J. G. Seo, *RSC Adv.*, 2015, **5**, 26197-26208.
23. X. Feng, C. Zhang, Y. Liu, X. Zuo and H. Shi, *Can. J. Chem. Eng.*, 2018, **75**, 2887-2892.
24. E. Kuhlmann, S. Himmler, H. Giebelhaus and P. Wasserscheid, *Green Chem.*, 2007, **9**, 233-242.
25. Z. B. Zhou, H. Matsumoto and K. Tatsumi, *Chem.-Eur. J.*, 2005, **10**, 6581-6591.
26. M. Chai, Y Jim, S. Fang, L. yang, S. I. Hirano and K. Tachibana, *J. Power Sources*, 2012, **216**, 323-329.
27. Z. B. Zhou, H. Matsumoto and K. Tatsumi, *Chem. Lett.*, 2004, **33**, 1636-1637.
28. M. M. Cecchini, C. Charnay, F. De Angelis, F. Lamaty, J. Martinez and E. Colacino, *Chemsuschem*, 2014, **7**, 45-65.
29. Y. D. Jin, S. H. Fang, M. Chai, L. Yang and S. Hirano, *Ind. Eng. Chem. Res.*, 2012, **51**, 11011-11020.
30. Z. Z. Yang, L. N. He, Q. W. Song, K. H. Chen, A. H. Liu and X. M. Liu, *Phys. Chem. Chem. Phys.*, 2012, **14**, 15832-15839.
31. S. K. Tang, G. A. Baker, S. Ravula, J. E. Jones and H. Zhao, *Green Chem.*, 2012, **14**, 2922-2932.
32. W. M. Liu, C. F. Ye, Q. Y. Gong, H. Z. Wang and P. Wang, *Tribol. Lett*, 2002, **13**, 81-85.
33. D. Qiao, H. Z. Wang and D. P. Feng, *Lubr. Sci.*, 2014, **26**, 1-11.
34. S. J. Zeng, J. Wang, L. Bai, B. Q. Wang, H. S. Gao, D. W. Shang, X. P. Zhang and S. J. Zhang, *Energy & Fuels*, 2015, **29**, 6039-6048.
35. C. Kolbeck, M. Killian, F. Maier, N. Paape, P. Wasserscheid and H.-P. Steinrück, *Langmuir*, 2008, **24**, 9500-9507.
36. B. S. J. Heller, C. Kolbeck, I. Niedermaier, S. Dommer, J. Schatz, P. Hunt, F. Maier and H.-P. Steinrück, *Chemphyschem*, 2018, **19**, 1733-1745.
37. Z. F. Fei, W. H. Ang, D. B. Zhao, R. Scopelliti, E. E. Zvereva, S. A. Katsyuba and P. J. Dyson, *J. Phys. Chem. B*, 2007, **111**, 10095-10108.

38. F. A. Hamprecht, A. J. Cohen, D. J. Tozer and N. C. Handy, *J. Chem. Phys.*, 1998, **109**, 6264-6271.
39. F. Jensen, *J. Chem.Theory Comput.*, 2015, **11**, 132-138.
40. N. A. Besley, A. T. B. Gilbert and P. M. W. Gill, *J. Chem. Phys.*, 2009, **130**.
41. J. P. Perdew, K. Burke and M. Ernzerhof, *Phys. Rev. Lett.*, 1996, **77**, 3865-3868.
42. A. E. A. Fouda and N. A. Besley, *Theor. Chem. Acc.*, 2017, **137**.
43. T. N. Truong and E. V. Stefanovich, *Chem. Phys. Lett.*, 1995, **240**, 253-260.
44. V. Barone and M. Cossi, *J. Phys. Chem. A*, 1998, **102**, 1995-2001.
45. M. Cossi, N. Rega, G. Scalmani and V. Barone, *J. Comput. Chem.*, 2003, **24**, 669-681.
46. C. D. Wagner, L. E. Davis, M. V. Zeller, J. A. Taylor, R. H. Raymond and L. H. Gale, *Surf. Interface Anal.*, 1981, **3**, 211-225.
47. I. J. Villar-Garcia, E. F. Smith, A. W. Taylor, F. L. Qiu, K. R. J. Lovelock, R. G. Jones and P. Licence, *Phys. Chem. Chem. Phys.*, 2010, **13**, 2797-2808.
48. Z. J. Chen, Y. N. Huo, J. Cao, L. Xu and S. G. Zhang, *Ind. Eng. Chem. Res.*, 2016, **55**, 11589-11596.
49. D. Briggs and G. Beamson, *Anal. Chem.*, 1993, **65**, 1517-1523.
50. J. L. Rivera, L. Molina-Rodriguez, M. Ramos-Estrada, P. Navarro-Santos and E. Lima, *RSC Adv.*, 2018, **8**, 10115-10123.
51. S. Zhang, X. Lu, Q. Zhou, X. Li, X. Zhang and S. Li, *Elsevier*, 2009, 1-478.
52. S. Tsuzuki, H. Tokuda, K. Hayamizu and M. Watanabe, *J. Phys. Chem. B*, 2005, **109**, 16474-16481.
53. K. R. Harris, T. Makino and M. Kanakubo, *Phys. Chem. Chem. Phys.*, 2014, **16**, 9161-9170.
54. J. H. Lee, J. B. Ryu, A. S. Lee, W. Na, H. S. Yoon, W. J. Kim and C. M. Koo, *Electrochim. Acta*, 2016, **222**, 1847-1852.
55. H. S. Schrekker, D. O. Silva, M. A. Gelesky, M. P. Stracke, C. M. L. Schrekker, R. S. Goncalves and J. Dupont, *J. Braz. Chem. Soc.*, 2008, **19**, 426-433.
56. K. Noack, P. S. Schulz, N. Paape, J. Kiefer, P. Wasserscheid and A. Leipertz, *Phys. Chem. Chem. Phys.*, 2010, **12**, 14153-14161.
57. T. Cremer, C. Kolbeck, K. R. J. Lovelock, N. Paape, R. Wölfel , P. S. Schulz, P. Wasserscheid, H. Weber, J. Thar, B. Kirchner, F. Maier and H.-P. Steinrück, *Chem. Eur. J*, 2010, **16**, 9018-9033.
58. J. Thar, M. Brehm, A. P. Seitsonen and B. Kirchner, *J. Phys. Chem. B*, 2009, **113**, 15129-15132.
59. F. Bernardi, J. D. Scholten, G. H. Fecher, J. Dupont and J. Morais, *Chem. Phys. Lett.*, 2009, **479**, 113-116.